BİTLİS EREN ÜNİVERSİTESİ
FEN BİLİMLERİ DERGİSİ

ISSN: 2147-3129 / e-ISSN: 2147-3188

Article Type : Research Article
Received : November 22, 2024
Revised : January 24, 2025
Accepted : February 12, 2025
DOI : 10.17798/bitlisfen.1589786

Year : 2025
Volume : 14
Issue : 1
Pages : 361-384

MODELING MONKEYPOX: SPREAD OF OUTBREAK WITH SOCIAL DISTANCING, QUARANTINE AND VACCINATION

Mahir Demir [1]

[1] *Giresun University, Department of Mathematics, Giresun, Türkiye, mahir.demir@giresun.edu.tr*

ABSTRACT

In this paper, we introduced a novel mathematical model to simulate the spread of the zoonotic viral disease monkeypox, incorporating both human and rodent populations to capture the disease dynamics. Unlike previous models, we included a quarantine compartment for infected humans, a social distancing compartment for susceptible individuals, and vaccination with direct transmission to the recovered compartment, offering a more comprehensive framework for controlling the spread of monkeypox. We then compared the effectiveness of these three control measures in reducing disease transmission. To investigate the dynamics of the model, we first demonstrated that it has a unique, positive, and bounded solution. Next, we calculated the basic reproduction number, R_0 for the proposed model. A sensitivity analysis is then conducted to identify key parameters, followed by an assessment of their effects on R_0. Additionally, we analyzed the local stability of both the disease-free and endemic equilibrium points to identify the conditions under which the disease dies out or remains endemic. We first showed in stability analysis section that these three control parameters play important roles in stability of equlibrium points. After that our findings in sensitivity analysis indicated the critical role of recovery rates and incubation periods in shaping the outbreak trajectory. Besides them, our analysis of R_0 in 3-D plots showed that the human-to-human transmission (β_{hh}) has about 3 times greater impact than rodent-to-human transmission (β_{rh}) on R_0. Finally, we presented simulations to show single and combined effects of the control parameters: quarantine, social distancing and vaccination on the transmission of monkeypox virus.

Keywords: Mpox, Sensitivity analysis, Infectious disease, Basic reproduction number, Stability analysis.

1 INTRODUCTION

Monkeypox is a zoonotic viral disease caused by the monkeypox virus, a member of the Orthopoxvirus genus, which also includes the smallpox virus. First identified in 1958 in laboratory monkeys, the disease is primarily transmitted to humans through direct contact with infected animals, particularly rodents, or through respiratory droplets and contaminated objects from human-to-human contact [1]. Symptoms typically include fever, headache, muscle aches, and swollen lymph nodes, followed by a characteristic rash that often begins on the face and spreads to other body parts. The incubation period ranges from 5 to 21 days, and while the disease is generally less severe than smallpox, it can still lead to complications and, in rare cases, death, with mortality rates varying by geographic region and viral strain [2], [3].

Various mathematical models have been employed to investigate the transmission dynamics of monkeypox, focusing on interactions among different population groups. [4] introduced a SIQR-SEI model to analyze rodent-to-human transmission, highlighting the role of quarantine in controlling infection spread. Another study developed a deterministic model incorporating vaccination to explore monkeypox dynamics, revealing that epidemic outcomes depend heavily on vaccination efficacy (categorized as weak, medium, or strong) [5]. Additionally, a study by authors [6] emphasized quarantine and public awareness campaigns as essential strategies for reducing human-to-human transmission. However, these studies often excluded the exposed (E) compartment in their frameworks, which limits their application to diseases with significant latent periods.

Conversely, other studies have included the exposed compartment to capture more realistic transmission dynamics. [7] applied an SEIR model with low-infectious and high-infectious compartments alongside quarantine measures. [8] extended this by incorporating a quarantine compartment for infected individuals, improving insights into isolation's effectiveness. Similarly, [9] expanded the SEIR framework with a compartment for vaccinated individuals and [13] expanded with isolated individuals to model monkeypox transmission comprehensively. A recent study by [10] analyzed SEIR-based frameworks, highlighting their utility in understanding human-animal transmission interactions and guiding public health interventions. These contributions demonstrate the growing reliance on SEIR models to better reflect the disease's natural history and control strategies.

Unlike other studies on monkeypox modeling, we did not include a separate compartment for vaccinated individuals. Instead, vaccinated individuals were directly moved

to the recovered compartment, assuming immunity acquisition based on vaccine efficacy and vaccination rates among susceptible individuals. By grouping vaccinated and recovered individuals, we simplified the model, reflecting their shared immune status. Given monkeypox's primary transmission via direct contact with infected fluids or objects, we assumed negligible infection risk within the isolated (social distancing) compartment and focused on high-risk interactions. Our model incorporated vaccination, social distancing, and quarantine to analyze their combined effects on monkeypox virus transmission. Such control measures are well studied on COVID-19 virus [24-27]. For instance, the effects of social distancing, quarantine, and lockdown on COVID-19 dynamics were carefully analyzed in the study presented by [24].

The recent spread of monkeypox beyond its usual regions has shown the need for effective strategies to control its spread. Measures like vaccination, social distancing, and quarantine are known to work well individually, but their combined effects are less understood. It is important to study how these measures interact, especially since public compliance with social distancing and quarantine can impact the success of vaccination efforts. Understanding how to combine these strategies effectively can help manage monkeypox outbreaks and improve readiness for future pandemics, ensuring public health responses are both efficient and flexible.

In the following section, we first introduced the compartmental model, identified its equilibrium points, and calculated the basic reproduction number, R_0. We then analyzed the stability of these equilibrium points. A sensitivity analysis was conducted using parameter values derived from previous studies to understand how variations in key factors affect the spread of monkeypox outbreak. In the result section, we presented plots illustrating how R_0 changes in response to variations in critical parameters identified through sensitivity analysis. Finally, we discussed the individual and combined impacts of quarantine, social distancing, and vaccination on controlling disease spread.

2 MATERIAL AND METHOD

In this study, to model the spread of the monkeypox virus, the human population was divided into six compartments, and the rodent population was divided into four compartments. The SEIQPR model was used to represent the human population and the SEIR model was used to represent the rodent population. For the transmission diagram of the disease between compartments, see Figure 1, and for the definitions of the compartments, see Table 1. The total human population was expressed as $N_h = S_h + E_h + I_h + Q_h + P_h + R_h$ and the rodent

population was expressed as $N_r = S_r + E_r + I_r + R_r$. We assumed that a vaccinated human gains immunity to the monkeypox virus, allowing them to transition directly to the recovered class. Since monkeypox mainly transmits through direct contact with infected fluids or contaminated objects, we assume that the infection risk is negligible in the social distancing compartment (P_h) and exclude transmission in this group, focusing instead on higher-risk interactions.

2.1 Model Formulation

We proposed a compartmental model that incorporates both human and rodent populations to describe monkeypox transmission dynamics, represented by the following system of differential equations:

$$\begin{aligned}
\frac{dS_h}{dt} &= \Lambda_h - (\beta_{hh} I_h + \beta_{rh} I_r) S_h - (d_h + b + v) S_h \\
\frac{dE_h}{dt} &= (\beta_h I_{hh} + \beta_{rh} I_r) S_h - (k_h + d_h) E_h \\
\frac{dI_h}{dt} &= k_h E_h - (q + \mu_{h_1} + d_h + \gamma_{h_1}) I_h \\
\frac{dQ_h}{dt} &= q I_h - (\mu_{h_2} + d_h + \gamma_{h_2}) Q_h \\
\frac{dP_h}{dt} &= b S_h - (v + d_h) P_h \\
\frac{dR_h}{dt} &= \gamma_{h_1} I_h + \gamma_{h_2} Q_h + v(S_h + P_h) - d_h R_h \\
\frac{dS_r}{dt} &= \Lambda_r - (\beta_{rr} I_r + \beta_{hr} I_h) S_r - d_r S_r \\
\frac{dE_r}{dt} &= (\beta_{rr} I_r + \beta_{hr} I_h) S_r - (k_r + d_r) E_r \\
\frac{dI_r}{dt} &= k_r E_r - (\mu_r + d_r + \gamma_r) I_r \\
\frac{dR_r}{dt} &= \gamma_r I_r - d_r R_r
\end{aligned} \tag{1}$$

where, $S_h(0) = S_{h,0}$, $E_h(0) = E_{h,0}$, $I_h(0) = I_{h,0}$, $Q_h(0) = Q_{h,0}$, $P_h(0) = P_{h,0}$, $R_h(0) = R_{h,0}$, $S_r(0) = S_{r,0}$, $E_r(0) = E_{r,0}$, $I_r(0) = I_{r,0}$ and $R_r(0) = R_{r,0}$ values represent the initial

conditions of the differential equation. That is, they express the number of individuals in each compartment at time $t = 0$. All these values are defined as non-negative real numbers with upper bounds. Similarly, all parameters defined in Table 2 are specified as positive real numbers with upper bounds. In the study, we mainly focused on the control parameters v (vaccination), b (social distancing), and q (quarantine) in the mitigation of monkeypox virus.

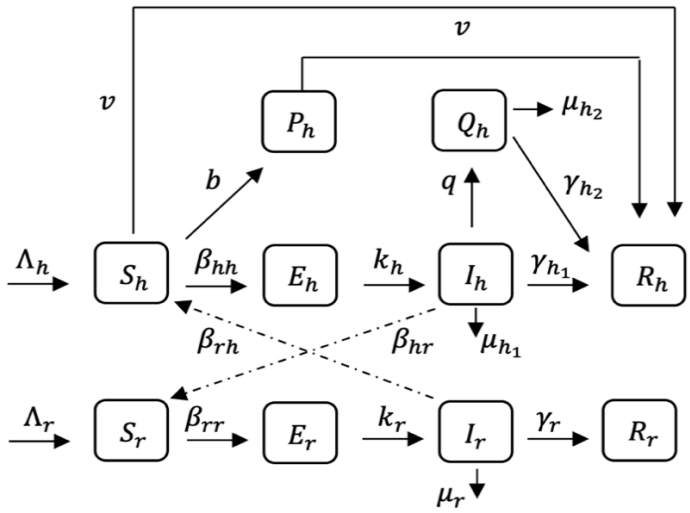

Figure 1. Flow diagram illustrating the disease transitions among the compartments.

Table 1. Population compartments and their descriptions.

Compartments	Descriptions	Initial densities of populations
S_r	Susceptible rodents	0.9990
E_r	Exposed rodents	0.0004
I_r	Infected rodents	0.0006
R_r	Recovered rodents	0.0000
S_h	Susceptible humans	0.9990
P_h	Social Distanced-Susceptible humans	0.0004
E_h	Exposed humans	0.0006
I_h	Infected humans	0.0000
Q_h	Quarantined-Infected humans	0.0000
R_h	Recovered humans	0.0000

Table 2. The model parameters, along with their descriptions and values in the time unit days. For the control parameters v, b, and q, we used a base value of 0.0001 and then varied them in result section to show their effects on the infected cases.

Parameters	Descriptions	Value ($\frac{1}{day}$)	Source
Λ_h	Recruitment rate of human population	-	-
d_h	Natural death rate of human population	-	-
β_{hh}	Disease transmission rate from humans to humans	0.3000	Assumed
β_{rh}	Disease transmission rate from rodents to humans	0.1500	Assumed
β_{rr}	Disease transmission rate from rodents to rodents	0.3000	Assumed
β_{hr}	Disease transmission rate from humans to rodents	0.1500	Assumed
v	(Vaccine efficacy rate) x (the percentage of vaccinated susceptible individuals)	0.0001	Assumed
b	Rate of transition to social distancing class from susceptible class	0.0001	Assumed
q	Rate of moving infected to quarantined-infected individuals	0.0001	Assumed
μ_{h_1}	Disease-induced death rate of human population in I_h	0.0033	[11]
μ_{h_2}	Disease-induced death rate of human population in Q_h	0.0555	[11]
k_h	Rate of exposed individuals becoming infected	0.0500	[12]
γ_{h_1}	Recovery rate due to natural immune response	0.0884	[11]
γ_{h_2}	Recovery rate due to hospitalization	0.0363	[11]
Λ_r	Recruitment rate of rodent population	-	-
d_r	Natural death rate of rodent population	-	-
k_r	Rate of exposed rodents becoming infected	0.3200	[12]
μ_r	Disease-induced death rate of rodent population	0.2814	[12]
γ_r	Recovery rate of rodents due to natural immune response	0.6000	[14]

Theorem 1. *Assuming that the initial conditions are defined in a region Ω, the system of differential equations given in (1) has a unique positive and bounded solution in the region Ω for each $t \in [0,T]$. Specifically,*

$$\Omega = \left\{(S_h, E_h, I_h, Q_h, P_h, R_h, S_r, E_r, I_r, R_r) \subset \mathbb{R}_+^{10} : 0 < N_h \leq \frac{\Lambda_h}{d_h}, 0 < N_r \leq \frac{\Lambda_r}{d_r}\right\}.$$

Proof. Let's first show boundedness of solutions for model (1)

$$\begin{aligned} \frac{dN_h}{dt} &= \frac{dS_h}{dt} + \frac{dE_h}{dt} + \frac{dI_h}{dt} + \frac{dQ_h}{dt} + \frac{dP_h}{dt} + \frac{dR_h}{dt} \\ &= \Lambda_h - d_h(S_h + E_h + I_h + Q_h + P_h + R_h) - \mu_{h_1} I_h - \mu_{h_2} Q_h \quad (2) \\ &\leq \Lambda_h - d_h(S_h + E_h + I_h + Q_h + P_h + R_h) \end{aligned}$$

$$\Longrightarrow \quad \frac{dN_h}{dt} \leq \Lambda_h - d_h N_h$$

$$\Longrightarrow \quad \limsup_{t \to \infty} N_h \leq \frac{\Lambda_h}{d_h}$$

If $\frac{dN_h}{dt}$ were positive, the solution would increase and go to infinity. Therefore, to prevent this increase, this derivative must take a maximum value of zero. In other words, if we want the solution to the differential equation system to remain within a boundary, the total number of individuals in the human population, $N_h(t)$, must either remain constant or decrease. Therefore, the derivative $\frac{dN_h}{dt}$ can be at most zero. Similarly, let us now demonstrate that the solution for the rodent population is also bounded:

$$\begin{aligned} \frac{dN_r}{dt} &= \frac{dS_r}{dt} + \frac{dE_r}{dt} + \frac{dI_r}{dt} + \frac{dR_r}{dt} \\ &= \Lambda_r - \mu_r I_r - d_r(S_r + E_r + I_r + R_r) \qquad (3) \\ &\leq \Lambda_r - d_r(S_r + E_r + I_r + R_r) \end{aligned}$$

$$\Longrightarrow \quad \frac{dN_r}{dt} \leq \Lambda_r - d_r N_r$$

$$\Longrightarrow \quad \limsup_{t\to\infty} N_r \leq \frac{\Lambda_r}{\mu_r}.$$

Thus, $N_h \leq \frac{\Lambda_h}{d_h}$ and $N_r \leq \frac{\Lambda_r}{\mu_r}$. Now, we show the positivity of the solutions. by using Eq. 2, we get following since $-\mu_h Q_h \geq -\mu_h N_h$.

$$\begin{aligned} \frac{dN_h}{dt} &= \Lambda_h - d_h(S_h + E_h + I_h + Q_h + P_h + R_h) - \mu_{h_1} I_h - \mu_{h_2} Q_h \\ &\geq \Lambda_h - d_h N_h - \mu_h N_h = \Lambda_h - (d_h + \mu_{h_1} + \mu_{h_2}) N_h \end{aligned}$$

By linearity of the differential equation, we can multiply the above inequality by the integral factor, $e^{\int_0^t (d_h+\mu_{h_1}+\mu_{h_2})ds} = e^{(d_h+\mu_{h_1}+\mu_{h_2})t}$ and obtain the following for $s \in (0,t)$

$$N_h e^{(d_h+\mu_{h_1}+\mu_{h_2})t} = N_{h,0} + \Lambda_h \int_0^t e^{(d_h+\mu_{h_1}+\mu_{h_2})s}\, ds > 0.$$

Thus, we obtained $0 < N_h \leq \frac{\Lambda_h}{d_h}$. Similarly, by using Eq. 3, we got the following as

$$\begin{aligned} \frac{dN_r}{dt} &= \Lambda_r - \mu_r I_r - d_r(S_r + E_r + I_r + R_r) \\ &\geq \Lambda_r - (\mu_r + d_r) N_r \end{aligned}$$

By linearity of the differential equation, we obtained

$$N_r e^{(\mu_r+d_r)t} \geq N_{r,0} + \Lambda_r \int_0^t e^{(\mu_r+d_r)s}\, ds > 0$$

Hence, $0 < N_h \leq \frac{\Lambda_h}{d_h}$ and $0 < N_r \leq \frac{\Lambda_r}{d_r}$.

2.2 Equilibrium Points of the Model

2.2.1 The disease-free equilibrium point and basic reproduction number (R_0)

The disease-free equilibrium is the state where no disease is present in the system ($I_r = I_h = 0$). Thus, the disease-free equilibrium of system (1) is given by

$$E_1 = (S_h^*, E_h^*, I_h^*, Q_h^*, P_h^*, R_h^*, S_r^*, E_r^*, I_r^*, R_r^*) = \left(\frac{\Lambda_h}{d_h}, 0,0,0,0, \frac{\Lambda_r}{d_r}, 0,0,0\right).$$

Thus, this indicates that susceptible humans and rodents will stay at the maximum level when there is no disease since $0 < N_h \leq \frac{\Lambda_h}{d_h}$ and $0 < N_r \leq \frac{\Lambda_r}{d_r}$.

While determining the basic reproduction number (R_0), the Next Generation Matrix Method will be used [15]. This matrix is based on two main components: The new infections matrix (F): This matrix shows the rates at which new cases emerge in the epidemic. The transition matrix (V): This matrix represents the transitions of individuals among the classes: E_h, I_h, Q_h, E_r and I_r. We get these matrices in the order $(E_h, I_h, Q_h, E_r, I_r)$ as follow:

$$F = \begin{bmatrix} (\beta_{hh} I_h + \beta_{rh} I_r) S_h \\ 0 \\ 0 \\ (\beta_{rr} I_r + \beta_{hr} I_h) S_r \\ 0 \end{bmatrix} \quad \text{and} \quad V = \begin{bmatrix} (d_h + k_h) E_h \\ -k_h E_h + (q + \mu_{h_1} + d_h + \gamma_{h_1}) I_h \\ -q I_h + (\mu_{h_2} + d_h + \gamma_{h_2}) Q_h \\ (k_r + d_r) E_r \\ -k_r E_r + (\mu_r + d_r + \gamma_r) I_r \end{bmatrix}$$

$$\mathcal{F} = \begin{bmatrix} 0 & \beta_{hh} S_h & 0 & 0 & \beta_{rh} S_h \\ 0 & 0 & 0 & 0 & 0 \\ 0 & 0 & 0 & 0 & 0 \\ 0 & \beta_{hr} S_r & 0 & 0 & \beta_{rr} S_r \\ 0 & 0 & 0 & 0 & 0 \end{bmatrix} = \begin{bmatrix} 0 & \beta_{hh} \frac{\Lambda_h}{d_h} & 0 & 0 & \beta_{rh} \frac{\Lambda_h}{d_h} \\ 0 & 0 & 0 & 0 & 0 \\ 0 & 0 & 0 & 0 & 0 \\ 0 & \beta_{hr} \frac{\Lambda_r}{d_r} & 0 & 0 & \beta_{rr} \frac{\Lambda_r}{d_r} \\ 0 & 0 & 0 & 0 & 0 \end{bmatrix}_{E_1}$$

$$\mathcal{V} = \begin{bmatrix} k_h + d_h & 0 & 0 & 0 & 0 \\ -k_h & q + \mu_{h_1} + d_h + \gamma_{h_1} & 0 & 0 & 0 \\ 0 & -q & \mu_{h_2} + d_h + \gamma_{h_2} & 0 & 0 \\ 0 & 0 & 0 & k_r + d_r & 0 \\ 0 & 0 & 0 & -k_r & (\mu_r + d_r + \gamma_r \end{bmatrix}_{E_1}$$

$$\mathcal{V}^{-1} = \begin{bmatrix} \frac{1}{k_h+d_h} & 0 & 0 & 0 & 0 \\ M_1 & \frac{1}{q+\mu_{h_1}+d_h+\gamma_{h_1}} & 0 & 0 & 0 \\ M_2 & \frac{q}{(q+\mu_{h_1}+d_h+\gamma_{h_1})(\mu_{h_2}+d_h+\gamma_{h_2})} & \frac{1}{\mu_{h_2}+d_h+\gamma_{h_2}} & 0 & 0 \\ 0 & 0 & 0 & \frac{1}{k_r+d_r} & 0 \\ 0 & 0 & 0 & \frac{k_r}{(k_r+d_r)(\mu_r+d_r+\gamma_r)} & \frac{1}{\mu_r+d_r+\gamma_r} \end{bmatrix}$$

where $M_1 = \frac{k_h}{(k_h+d_h)(q+\mu_{h_1}+d_h+\gamma_{h_1})}$ and $M_2 = \frac{qk_h}{(k_h+d_h)(q+\mu_{h_1}+d_h+\gamma_{h_1})(\mu_{h_2}+d_h+\gamma_{h_2})}$. By multiplying the matrices $\mathcal{F}$ *and* $\mathcal{V}^{-1}$, we got the following

$$\mathcal{F}\mathcal{V}^{-1} = \begin{bmatrix} \frac{\beta_{hh}\Lambda_h k_h}{d_h(k_h+d_h)(q+\mu_{h_1}+d_h+\gamma_{h_1})} & \frac{\beta_{hh}\Lambda_h}{d_h(q+\mu_{h_1}+d_h+\gamma_{h_1})} & 0 & \frac{\beta_{rh}\Lambda_h k_r}{d_h(k_r+d_r)(\mu_r+d_r+\gamma_r)} & \frac{\beta_{rh}\Lambda_h}{d_h(\mu_r+d_r+\gamma_r)} \\ 0 & 0 & 0 & 0 & 0 \\ 0 & 0 & 0 & 0 & 0 \\ \frac{\beta_{hr}\Lambda_r k_h}{d_r(k_h+d_h)(q+\mu_{h_1}+d_h+\gamma_{h_1})} & \frac{\beta_{hr}\Lambda_h}{d_r(q+\mu_{h_1}+d_h+\gamma_{h_1})} & 0 & \frac{\beta_{rr}\Lambda_r k_r}{d_r(k_r+d_r)(\mu_r+d_r+\gamma_r)} & \frac{\beta_{rr}\Lambda_r}{d_r(\mu_r+d_r+\gamma_r)} \\ 0 & 0 & 0 & 0 & 0 \end{bmatrix}$$

$$R_0^{hh} = \frac{\beta_{hh}\Lambda_h k_h}{d_h(k_h+d_h)(q+\mu_{h_1}+d_h+\gamma_{h_1})}, \quad R_0^{rh} = \frac{\beta_{rh}\Lambda_h k_r}{d_h(k_r+d_r)(\mu_r+d_r+\gamma_r)}$$

$$R_0^{hr} = \frac{\beta_{hr}\Lambda_r k_h}{d_r(k_h+d_h)(q+\mu_{h_1}+d_h+\gamma_{h_1})}, \quad R_0^{rr} = \frac{\beta_{rr}\Lambda_r k_r}{d_r(k_r+d_r)(\mu_r+d_r+\gamma_r)}$$

Here, R_0^{hh} and R_0^{rr} are the basic reproduction numbers for human-to-human, rodents-to-rodents transmission, while R_0^{hr} and R_0^{rh} are the basic reproduction numbers for the vectorial transmissions from human-to-rodent and rodent-to-human, respectively. Thus, the basic reproduction number for model (1) is a composition of the reproduction numbers as follows (see the studies for details: [16] and [17]). Shortly, when we arrange the characteristic polynomial of $\mathcal{F}\mathcal{V}^{-1}$ matrix and arrange it, we will get the following, which is the maximum eigenvalue of the matrix.

$$R_0 = \frac{1}{2}\left\{(R_0^{hh} + R_0^{rr}) + \sqrt{(R_0^{hh} + R_0^{rr})^2 - 4(R_0^{hh}R_0^{rr} - R_0^{hr}R_0^{rh})}\right\}$$

when we simplify the equation, we obtain

$$R_0 = \frac{1}{2}\left\{(R_0^{hh} + R_0^{rr}) + \sqrt{(R_0^{hh} - R_0^{rr})^2 + 4R_0^{hr}R_0^{rh}}\right\} \tag{4}$$

Thus, any changes in these reproduction numbers affect the basic reproduction number, R_0.

2.2.2 Endemic equilibrium

This is the equilibrium where the disease stays in the system when $R_0 > 1$. See Theorem 4 for the existence of the endemic equilibrium point.

Theorem 2. *When $I_r > 0$, there is at least one endemic equilibrium point for the system given in equation (1).*

Proof. Suppose that $I_r > 0$. Setting $\frac{dI_r}{dt} = 0$ and $\frac{dR_r}{dt} = 0$, we obtained

$$E_r = \frac{\mu_r + d_r + \gamma_r}{k_r} I_r \tag{5}$$

$$R_r = \frac{\gamma_r}{d_r} I_r \tag{6}$$

when we set $\frac{dS_r}{dt} + \frac{dE_r}{dt} = 0$, we obtained

$$S_r = \frac{\Lambda_r - (k_r + d_r)E_r}{d_r} \tag{7}$$

Since $N_r = S_r + E_r + I_r + R_r$, $I_r = N_r - S_r - E_r - R_r$ and we got the following by using the equations (5-7)

$$I_r^* = \frac{\Lambda_r - d_r N_r}{\mu_r} \tag{8}$$

Hence,

$$S_r^* = \frac{\Lambda_r - (k_r + d_r)E_r}{d_r} = \frac{\Lambda_r}{d_r} - \frac{(k_r + d_r)(\mu_r + d_r + \gamma_r)}{d_r k_r} \frac{\Lambda_r - d_r N_r}{\mu_r} \tag{9}$$

$$E_r^* = \frac{\mu_r + d_r + \gamma_r}{k_r} \frac{\Lambda_r - d_r N_r}{\mu_r} \quad \text{and} \quad R_r^* = \frac{\gamma_r}{d_r} \frac{\Lambda_r - d_r N_r}{\mu_r} \tag{10}$$

Similarly, by setting $\frac{dI_h}{dt} = 0$, $\frac{dQ_h}{dt} = 0$, $\frac{dP_h}{dt} = 0$ and $\frac{dR_h}{dt} = 0$,

$$E_h = \frac{q + \mu_{h_1} + d_h + \gamma_{h_1}}{k_h} I_h, \qquad Q_h = \frac{q}{\mu_{h_2} + d_h + \gamma_{h_2}} I_h, \qquad S_h = \frac{v + d_h}{b} P_h \tag{11}$$

$$R_h = \frac{\gamma_{h_1} I_h + \gamma_{h_2} Q_h + v(S_h + P_h)}{d_h} = \frac{\gamma_{h_1} I_h}{d_h} + \frac{\gamma_{h_2} Q_h}{d_h} + \frac{v(d_h + b + v)}{v + d_h} S_h \tag{12}$$

As we set $\frac{dS_h}{dt} + \frac{dE_h}{dt} = 0$, then

$$S_h = \frac{\Lambda_h-(k_h+d_h)E_h}{d_h+b+v} = \frac{\Lambda_h-\frac{(k_h+d_h)(q+\mu_{h_1}+d_h+\gamma_{h_1})}{k_h}I_h}{d_h+b+v} \quad (13)$$

Since $N_h = S_h + E_h + I_h + Q_h + P_h + R_h$, $I_h = N_h - S_h - E_h - Q_h - P_h - R_h$ and we got the following by using the equations (11-13)

$$I_h^* = \frac{N_h-\frac{(v+1)\Lambda_h}{v+d_h}}{1-\frac{(v+1)(k_h+d_h)(q+\mu_{h_1}+d_h+\gamma_{h_1})}{(v+d_h)k_h}+\frac{q+\mu_{h_1}+d_h+\gamma_{h_1}}{k_h}+\frac{\gamma_{h_1}}{d_h}+\frac{q(d_h+\gamma_{h_2})}{d_h(\mu_{h_2}+d_h+\gamma_{h_2})}} \quad (14)$$

Hence, the endemic equilibrium point, $E_2 = (S_h^*, E_h^*, I_h^*, Q_h^*, P_h^*, R_h^*, S_r^*, E_r^*, I_r^*, R_r^*)$ was obtained as

$$S_h^* = \frac{\Lambda_h-\frac{(k_h+d_h)(q+\mu_{h_1}+d_h+\gamma_{h_1})}{k_h}I_h^*}{d_h+b+v},$$

$$E_h^* = \frac{q+\mu_{h_1}+d_h+\gamma_{h_1}}{k_h}I_h^*,$$

$$I_h^* = \frac{N_h-\frac{(v+1)\Lambda_h}{v+d_h}}{1-\frac{(v+1)(k_h+d_h)(q+\mu_{h_1}+d_h+\gamma_{h_1})}{(v+d_h)k_h}+\frac{q+\mu_{h_1}+d_h+\gamma_{h_1}}{k_h}+\frac{\gamma_{h_1}}{d_h}+\frac{q(d_h+\gamma_{h_2})}{d_h(\mu_{h_2}+d_h+\gamma_{h_2})}},$$

$$Q_h^* = \frac{q}{\mu_{h_2}+d_h+\gamma_{h_2}}I_h^*,$$

$$P_h^* = \frac{v+d_h}{b}S_h^* = \frac{v+d_h}{b}\frac{\Lambda_h-\frac{(k_h+d_h)(q+\mu_{h_1}+d_h+\gamma_{h_1})}{k_h}I_h^*}{d_h+b+v},$$

$$R_h^* = \frac{\gamma_{h_1}}{d_h}I_h^* + \frac{\gamma_{h_2}}{d_h}Q_h^* + \frac{v(d_h+b+v)}{v+d_h}S_h^* = \frac{v\Lambda_h}{v+d_h} + \left(\frac{\gamma_{h_1}}{d_h}+\frac{\gamma_{h_2}q}{d_h(\mu_{h_2}+d_h+\gamma_{h_2})}-\frac{v(k_h+d_h)(q+\mu_{h_1}+d_h+\gamma_{h_1})}{k_h(v+d_h)}\right)I_h^*,$$

$$S_r^* = \frac{\Lambda_r}{d_r} - \frac{(k_r+d_r)(\mu_r+d_r+\gamma_r)}{d_r k_r}\frac{\Lambda_r-d_r N_r}{\mu_r},$$

$$E_r^* = \frac{\mu_r+d_r+\gamma_r}{k_r}\frac{\Lambda_r-d_r N_r}{\mu_r},$$

$$I_r^* = \frac{\Lambda_r-d_r N_r}{\mu_r},$$

$$R_r^* = \frac{\gamma_r}{d_r}\frac{\Lambda_r-d_r N_r}{\mu_r}.$$

2.3 Stability Analysis of Equilibrium Points

In this section, we examined the stability analyses at the equilibrium points. In our model, once individuals reach the R_h or R_r class, they are no longer involved in the disease transmission process. They are assumed immune and do not contribute to future infections, meaning their behavior does not affect the ongoing dynamics of infection spread or disease stability. To reduce the complexity and calculation in stability analysis, we excluded these

classes. Thus, we calculated the Jacobian matrix of the differential equation system (1) in the order $(S_h, E_h, I_h, Q_h, P_h, S_r, E_r, I_r)$ as follows:

$$J = \begin{bmatrix} a_{11} & 0 & a_{13} & 0 & 0 & 0 & 0 & a_{18} \\ a_{21} & a_{22} & a_{23} & 0 & 0 & 0 & 0 & a_{28} \\ 0 & a_{32} & a_{33} & 0 & 0 & 0 & 0 & 0 \\ 0 & 0 & a_{43} & a_{44} & 0 & 0 & 0 & 0 \\ a_{51} & 0 & 0 & 0 & a_{55} & 0 & 0 & 0 \\ 0 & 0 & 0 & 0 & 0 & a_{66} & 0 & a_{68} \\ 0 & 0 & 0 & 0 & 0 & a_{76} & a_{77} & a_{78} \\ 0 & 0 & 0 & 0 & 0 & 0 & a_{87} & a_{88} \end{bmatrix}$$

where,

$a_{11} = -(\beta_{hh} I_h + \beta_{rh} I_r) - (d_h + b + v)$, $a_{13} = -\beta_{hh} S_h$, $a_{18} = -\beta_{rh} S_h$, $a_{21} = \beta_{hh} I_h + \beta_{rh} I_r$, $a_{22} = -(k_h + d_h)$, $a_{23} = \beta_{hh} S_h$, $a_{28} = \beta_{rh} S_h$, $a_{32} = k_h$, $a_{33} = -\left(q + \mu_{h_1} + d_h + \gamma_{h_1}\right)$, $a_{43} = q$, $a_{44} = -\left(\mu_{h_2} + d_h + \gamma_{h_2}\right)$, $a_{51} = b$, $a_{55} = -(v + d_h)$, $a_{66} = -\beta_{rr} I_r - d_r$, $a_{68} = -\beta_{rr} S_r$, $a_{76} = \beta_{rr} I_r$, $a_{77} = -(k_r + d_r)$, $a_{78} = \beta_{rr} S_r$, $a_{87} = k_r$, $a_{88} = -(\mu_r + d_r + \gamma_r)$.

Theorem 3. *The disease-free equilibrium point is asymptotically local stable if the conditions* $1 > R_0^{rr}$ *and* $1 > R_0^{hh}$ *are hold. Otherwise, it is unstable.*

Proof. The Jacobian matrix of the disease-free equilibrium point,

$$E_1 = (S_h^*, E_h^*, I_h^*, Q_h^*, P_h^*, , S_r^*, E_r^*, I_r^*) = \left(\frac{\Lambda_h}{d_h}, 0,0,0,0, \frac{\Lambda_r}{d_r}, 0,0\right).$$

was calculated as

$$J_{E_1} = \begin{bmatrix} a_{11} - \lambda & 0 & a_{13} & 0 & 0 & 0 & 0 & a_{18} \\ 0 & a_{22} - \lambda & a_{23} & 0 & 0 & 0 & 0 & a_{28} \\ 0 & a_{32} & a_{33} - \lambda & 0 & 0 & 0 & 0 & 0 \\ 0 & 0 & a_{43} & a_{44} - \lambda & 0 & 0 & 0 & 0 \\ a_{51} & 0 & 0 & 0 & a_{55} - \lambda & 0 & 0 & 0 \\ 0 & 0 & 0 & 0 & 0 & a_{66} - \lambda & 0 & a_{68} \\ 0 & 0 & 0 & 0 & 0 & 0 & a_{77} - \lambda & a_{78} \\ 0 & 0 & 0 & 0 & 0 & 0 & a_{87} & a_{88} - \lambda \end{bmatrix}$$

and its characteristic polynomial was obtained from $\left|J_{E_1} - \lambda I_{8x8}\right| = 0$ as

$$(a_{66} - \lambda)[(a_{88} - \lambda)(a_{77} - \lambda) - a_{87} a_{78}]$$

$$(a_{55} - \lambda)(a_{44} - \lambda)(a_{11} - \lambda)[(a_{33} - \lambda)(a_{22} - \lambda) - a_{32} a_{23}] = 0$$

The eigenvalues, $\lambda_1 = a_{11} = -\left(\mu_{h_2} + d_h + \gamma_{h_2}\right)$, $\lambda_2 = a_{44} = -\left(\mu_{h_2} + d_h + \gamma_{h_2}\right)$, $\lambda_3 = a_{55} = -(v + d_h)$ and $\lambda_4 = a_{66} = -d_r$, are negative.

$$[(a_{88}-\lambda)(a_{77}-\lambda)-a_{87}a_{78}]=0$$

$\Leftrightarrow$

$$\lambda^2-(a_{77}+a_{88})\lambda+a_{77}a_{88}-a_{87}a_{78}=0.$$

If $a_{77}a_{88}>a_{87}a_{78}$, then the eigenvalues are negative by Routh-Hurwitz Criteria (Routh, 1877; Hurwitz, 1895).

$$a_{77}a_{88}>a_{87}a_{78} \Leftrightarrow (k_r+d_r)(\mu_r+d_r+\gamma_r> k_r\beta_{rr}S_r$$

$$\Leftrightarrow 1>\frac{\beta_{rr}\Lambda_r k_r}{d_r(k_r+d_r)(\mu_r+d_r+\gamma_r)}=R_0^{rr}$$

Similarly, for the following equation

$$[(a_{33}-\lambda)(a_{22}-\lambda)-a_{32}a_{23}]=0$$

$\Leftrightarrow$

$$\lambda^2-(a_{22}+a_{33})\lambda+a_{22}a_{33}-a_{32}a_{23}=0$$

when $a_{22}a_{33}>a_{32}a_{23}$, the eigenvalues are negative by Routh-Hurwitz Criteria [18],[19].

$$a_{22}a_{33}>a_{32}a_{23} \Leftrightarrow (k_h+d_h)\left(q+\mu_{h_1}+d_h+\gamma_{h_1}\right)>k_h\beta_{hh}S_h$$

$$\Leftrightarrow 1>\frac{\beta_{hh}\Lambda_h k_h}{d_h(k_h+d_h)(q+\mu_{h_1}+d_h+\gamma_{h_1})}=R_0^{hh}$$

Thus, under the following conditions, the disease-free equilibrium is stable.

$$1>R_0^{rr} \tag{15}$$

$$1>R_0^{hh} \tag{16}$$

Theorem 4. *Under conditions (17) and (18), the endemic equilibrium point is asymptotically local stable. Otherwise, it is unstable.*

Proof. Let's set the Jacobian matrix of the endemic equilibrium point in the form $\left|J_{E_2}-\lambda I_{8x8}\right|=0$ as

$$J_{E_2}=\begin{bmatrix} a_{11}-\lambda & 0 & a_{13} & 0 & 0 & 0 & 0 & a_{18} \\ a_{21} & a_{22}-\lambda & a_{23} & 0 & 0 & 0 & 0 & a_{28} \\ 0 & a_{32} & a_{33}-\lambda & 0 & 0 & 0 & 0 & 0 \\ 0 & 0 & a_{43} & a_{44}-\lambda & 0 & 0 & 0 & 0 \\ a_{51} & 0 & 0 & 0 & a_{55}-\lambda & 0 & 0 & 0 \\ 0 & 0 & 0 & 0 & 0 & a_{66}-\lambda & 0 & a_{68} \\ 0 & 0 & 0 & 0 & 0 & a_{76} & a_{77}-\lambda & a_{78} \\ 0 & 0 & 0 & 0 & 0 & 0 & a_{87} & a_{88}-\lambda \end{bmatrix}$$

and then get the characteristic polynomial of the matrix,

$$[(a_{88}-\lambda)(a_{77}-\lambda)(a_{66}-\lambda)-a_{87}a_{78}(a_{66}-\lambda)+a_{87}a_{76}a_{68}](a_{55}-\lambda)(a_{44}-\lambda)$$

$$[(a_{33}-\lambda)(a_{22}-\lambda)(a_{11}-\lambda)-a_{32}a_{23}(a_{11}-\lambda)+a_{32}a_{21}a_{13}]=0$$

The eigenvalues, $\lambda_1 = a_{44} = -\left(\mu_{h_2} + d_h + \gamma_{h_2}\right)$ and $\lambda_2 = a_{55} = -(v + d_h)$ are negative. Now, we examine the other eigenvalues as

$$[(a_{88}-\lambda)(a_{77}-\lambda)(a_{66}-\lambda)-a_{87}a_{78}(a_{66}-\lambda)+a_{87}a_{76}a_{68}]=0$$

$\Leftrightarrow$

$$a_3\lambda^3 + a_2\lambda^2 + a_1\lambda + a_0 = 0$$

where, $a_3 = 1 > 0$, $a_2 = -(a_{66} + a_{77} + a_{88}) > 0$, $a_1 = -a_{87}a_{78} + a_{77}a_{88} + a_{66}(a_{77} + a_{88})$ and $a_0 = -a_{66}a_{77}a_{88} - a_{87}a_{76}a_{68} + a_{87}a_{78}a_{66}$. If $a_0, a_1 > 0$ and $a_2a_1 > a_3a_0$, then the eigenvalues are negative. Similarly, for the following equation

$$[(a_{33}-\lambda)(a_{22}-\lambda)(a_{11}-\lambda)-a_{32}a_{23}(a_{11}-\lambda)+a_{32}a_{21}a_{13}]=0$$

$\Leftrightarrow$

$$b_3\lambda^3 + b_2\lambda^2 + b_1\lambda + b_0 = 0$$

where, $b_3 = 1 > 0$, $b_2 = -(a_{11} + a_{22} + a_{33}) > 0$, $b_1 = -a_{32}a_{23} + a_{22}a_{33} + a_{11}(a_{22} + a_{33})$ and $b_0 = -a_{11}a_{22}a_{33} - a_{32}a_{21}a_{13} + a_{32}a_{23}a_{11}$. If $b_0, b_1 > 0$ and $b_2b_1 > b_3b_0$, then the eigenvalues are negative by Routh-Hurwitz Criteria. Thus, under the following conditions, the endemic equilibrium is stable.

$$a_0,\ a_1 > 0 \text{ and } a_2a_1 > a_3a_0 \tag{17}$$

$$b_0,\ b_1 > 0 \text{ and } b_2b_1 > b_3b_0 \tag{18}$$

3 RESULTS AND DISCUSSION

We presented and discussed model outputs in this section. It is important to emphasize that while we included the demographic parameters Λ_h, d_h, Λ_r and d_r in our analyses, they were not considered in the simulations. These parameters were utilized primarily to establish bounds on the model solutions in Section 2. Since these parameters pertain to the natural birth and death rates of specific populations and have no direct role in controlling infectious diseases, they are typically excluded in most infectious disease modeling frameworks [20], [21], [22].

This approach reflects the general practice of focusing on parameters directly influencing disease transmission and progression.

3.1 Stability Analysis

We investigate the stability of the disease-free equilibrium and endemic equilibrium points by using the parameter values given in Table 2. First, it is important to mention that since we are not including the demographic parameters, R_0 will be in the form:

$$R_0 = \frac{1}{2}\left\{(R_0^{hh} + R_0^{rr}) + \sqrt{(R_0^{hh} - R_0^{rr})^2 + 4R_0^{hr}R_0^{rh}}\right\} \tag{19}$$

where $$R_0^{hh} = \frac{\beta_{hh}}{(q+\mu_{h_1}+d_h+\gamma_{h_1})}, \quad R_0^{rh} = \frac{\beta_{rh}}{(\mu_r+d_r+\gamma_r)} \tag{20}$$

$$R_0^{hr} = \frac{\beta_{hr}}{(q+\mu_{h_1}+d_h+\gamma_{h_1})}, \quad R_0^{rr} = \frac{\beta_{rr}}{(\mu_r+d_r+\gamma_r)} \tag{21}$$

and the disease-free equilibrium point will be in the form:

$$E_1 = (S_h^*, E_h^*, I_h^*, Q_h^*, P_h^*, R_h^*, S_r^*, E_r^*, I_r^*, R_r^*) = (1,0,0,0,0,0,1,0,0,0).$$

rather than

$$E_1 = (S_h^*, E_h^*, I_h^*, Q_h^*, P_h^*, R_h^*, S_r^*, E_r^*, I_r^*, R_r^*) = \left(\frac{\Lambda_h}{d_h}, 0,0,0,0,0, \frac{\Lambda_r}{d_r}, 0,0,0\right).$$

Depending on our calculation by using parameter values given in Table 2, $R_0^{hh} = 3.26 > 1$ and $R_0^{rr} = 0.34 < 1$. Having, $R_0^{hh} = 3.26 > 1$ violate the stability of the disease-free equilibrium point (see Theorem 3). Thus, the disease-free equilibrium point is unstable. This finding highlights the need for additional efforts to control the outbreak. Specifically, incorporating control parameters v, b, and q is essential to reducing R_0^{hh} and mitigating transmission rates. Similarly, when we investigated the endemic equilibrium point with the parameter values given in Table 2, we obtained followings

$$a_3 = 1 > 0$$
$$a_2 = 1.2014 + 0.3I_r > 0$$
$$a_1 = -0.096S_r + 0.36I_r + 0.28 > 0.$$
$$a_0 = 0.0846I_r > 0.$$

and so, the condition (17) in Theorem 4 holds

$$a_0,\ a_1 > 0 \text{ and } a_2a_1 > a_3a_0$$

since we obtained

$$a_2a_1 > a_3a_0$$

$$\Leftrightarrow \quad 0.3364 + 0.4325I_r - 0.1153S_r > 0.0846I_r$$

Even assuming $S_r \cong 1$ and $I_r \cong 0$, which are the extreme cases, the inequality still holds. Thus, the condition (17) in Theorem 4 holds. Now, let investigate the condition (18) in Theorem 4. If this condition holds, then endemic equilibrium point is stable otherwise unstable. We obtained the following

$$b_3 = 1 > 0$$

$$b_2 = 0.3I_h + 0.15I_r + 0.1427 + v + b + q > 0$$

$$b_1 = -0.015S_h + 0.05q + 0.0046 + (0.3I_h + 0.15I_r + b + v)(q + 0.1417)$$

$$b_0 = 0.05(0.3I_h + 0.15I_r + b + v)(q + 0.0917) + 0.015S_h(0.3I_h + 0.15I_r + b + v)$$
$$+0.015S_h(0.3I_h + 0.15I_r) > 0$$

It is challenging to determine whether the condition $b_2b_1 > b_3b_0$ holds with the given parameters in Table 2, as it also requires identifying the variables S_h, I_h, and I_r and the control parameters v, b, and q. While this could be investigated numerically, such an analysis falls outside the scope of this study. However, we emphasize that the control parameters (v, b, and q) play a crucial role in the stability of the endemic equilibrium point. In the following sections, we examine the effects of these control parameters to highlight their significance in mitigating monkeypox outbreaks.

3.2 Sensitivity Analysis

Several parameters significantly influence the behavior of the model (1). To identify the parameters most relevant to the infected cases ($I_h + Q_h$), we performed a sensitivity analysis. This analysis employed Latin Hypercube Sampling (LHS) combined with the Partial Rank Correlation Coefficients (PRCC) method, following the approach described by [23]. Using parameter ranges provided in Table 3, we generated samples from a uniform distribution and used these as inputs to simulate system (1) over 150 days. The final number of infected cases served as the output variable for this analysis. Table 3 presents the PRCC values, associated p-values, and the parameter ranges used.

The results highlight v, b, q, β_{hh}, k_h, γ_{h_1} , γ_{h_2}, μ_r and γ_r as statistically significant parameters based on their high PRCC values, suggesting they play a pivotal role in outbreak dynamics. Consequently, we further analyzed how varying v, b, q, and β_{hh} affects the infected cases while keeping all other parameters fixed as listed in Table 2 and maintaining the initial

conditions in Table 1. Figures 2a-2d illustrate these findings, showing how the cumulative cases at the end of the simulation period respond to changes in these key parameters.

This investigation demonstrated that the control parameters v (vaccination) and b (social distancing) have nearly identical impacts on controlling the outbreak (see Figures 2a and 2b). This similarity is expected, as both parameters serve to reduce the spread of the disease in similar implementation in our model. In the absence of vaccination, implementing and managing social distancing measures can play a crucial role in mitigating monkeypox outbreaks.

The analysis also revealed that the recovery rates in the model play a critical role in controlling the outbreak, as they are statistically significant parameters. Additionally, the incubation period parameter (k_h) was identified as influential. Therefore, to effectively manage monkeypox outbreaks, it is essential to carefully examine this parameter to gain a better understanding of the disease dynamics.

Table 3. Results of sensitivity analysis with partial rank correlation coefficient (PRCC), p-value, and the parameter ranges used for calculations of the PRCC and p-values.

Parameters	Descriptions	PRCC	*p*-value	Parameter Ranges
v	(Vaccine efficacy rate) x (the percentage of vaccinated susceptible individuals)	-0.65	$9.3e^{-16}$	0.0001-0.1
b	Rate of transition to social distancing class from susceptible class	-0.63	$2.6e^{-15}$	0.0001-0.1
q	Rate of moving infected to quarantined-infected individuals	-0.48	$5.1e^{-10}$	0.001-0.3
β_{hh}	Disease transmission rate from humans to humans	0.55	$1.7e^{-12}$	0.01-1
β_{rh}	Disease transmission rate from rodents to humans	0.20	0.05	0.01-1
β_{rr}	Disease transmission rate from rodents to rodents	0.17	0.08	0.01-1
β_{hr}	Disease transmission rate from humans to rodents	0.07	0.5	0.01-1
μ_{h_1}	Disease-induced death rate of human population in I_h	-0.20	0.05	0.0001-0.1
μ_{h_2}	Disease-induced death rate of human population in Q_h	-0.24	0.02	0.0001-0.1
k_h	Rate of exposed individuals becoming infected	-0.61	$1.9e^{-14}$	0.001-1
γ_{h_1}	Recovery rate due to natural immune response	-0.36	0.0002	0.001-0.5
γ_{h_2}	Recovery rate due to hospitalization	-0.66	$1.5e^{-16}$	0.001-0.5
k_r	Rate of exposed rodents becoming infected	0.04	0.7	0.01-1
μ_r	Disease-induced death rate of rodent population	-0.28	0.004	0.01-1
γ_r	Recovery rate of rodents due to natural immune response	-0.35	0.0003	0.01-2

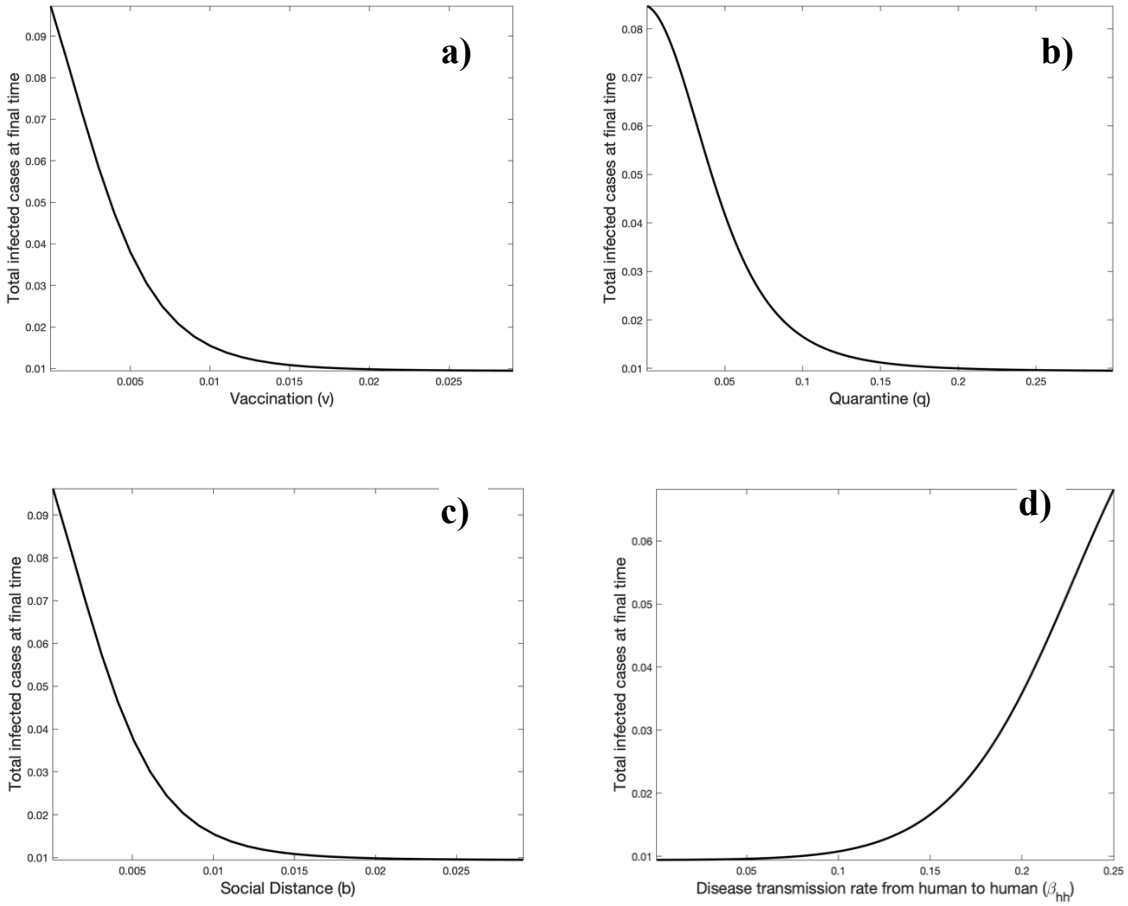

Figure 2. The total infected cases ($I_h + Q_h$) at the final time with respect to control parameters: vaccination (a), quarantine (b), social distance (c), and the disease transmission rate (d).

3.3 Analysis of Basic Reproduction Number, R_0

We investigated the changes on the basic reproduction number, R_0 depending on some of the important parameters presented by our sensitivity analysis in the previous subsection. We investigated the effect of the parameters $\gamma_{h_1}, q, \beta_{rh}$ and β_{hh} on R_0 while keeping all other parameters fixed as listed in Table 2. This investigation revealed that improving treatment quality to accelerate the recovery of infected individuals can significantly aid in mitigating the outbreak. Similarly, the rapid identification of infected individuals is equally crucial in controlling the spread of the disease (see Figure 3a).

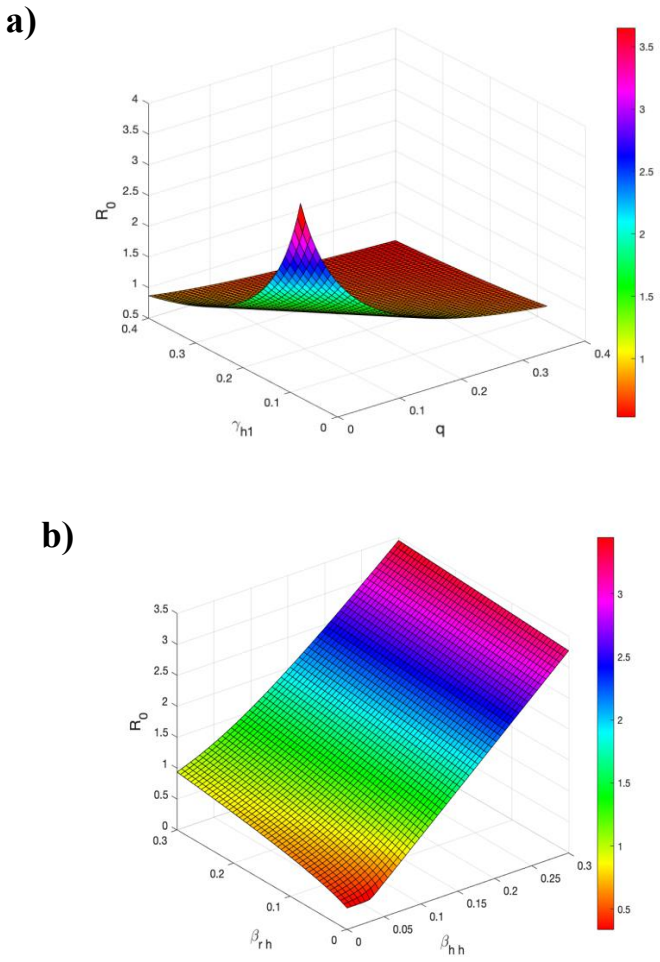

Figure 3. Surface plots of R_0. Plot a: showing the simultaneous impact of γ_{h_1} and q on R_0. Plot b: showing the simultaneous impact of β_{rh} and β_{hh} on R_0.

Our analysis also highlighted the significant influence of the parameter β_{hh} (human-to-human transmission) on the number of infected cases, compared to β_{rh} (rodent-to-human transmission). Notably, the human-to-human transmission was found to be nearly three times more impactful than the rodent-to-human transmission on the basic reproduction number (R_0) of the monkeypox virus (see Figure 3b).

3.4 Effects of Control Parameters on Infected Cases

As noted in the sensitivity analysis subsection (Figure 2), the control parameters *v* (vaccination) and *b* (social distancing) exhibit nearly identical effects on the number of infected cases. In Figure 4a, varying the parameters *v* or *b* between 0.0001 and 0.01 results in a similar reduction in infected cases, as indicated in the legend. However, applying both controls simultaneously leads to a substantially greater reduction in the infected cases, as demonstrated in Figure 4b.

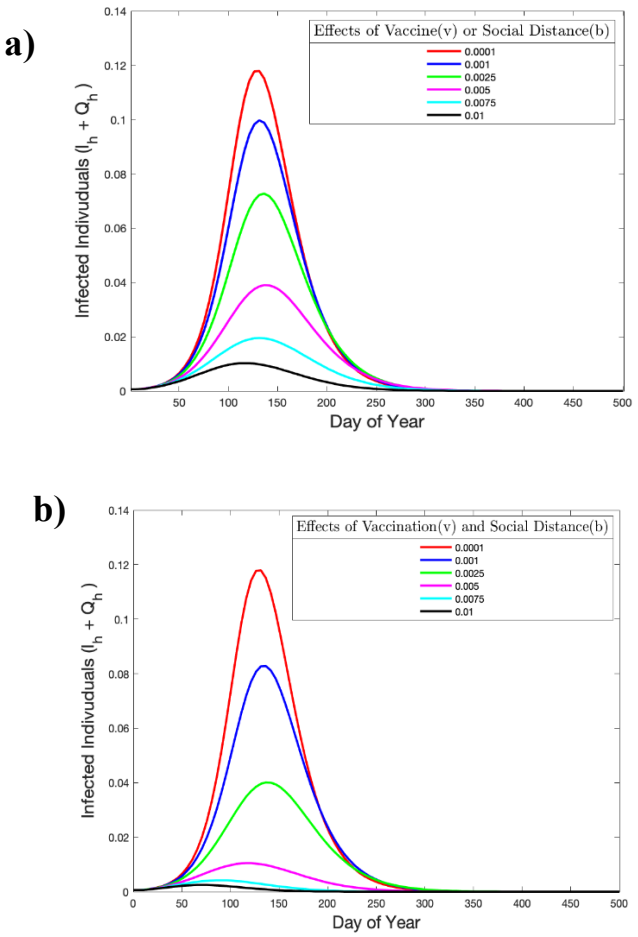

Figure 4. Effects of vaccination and /or social distancing on Infected cases. Plot a: the effect of vaccination or social distancing on the infected cases. Plot b: simultaneous effect of vaccination and social distancing on the infected cases.

When we applied only the quarantine parameter (q) to observe its effect on the infected cases, a noticeable shift in the peak of the infected cases curve emerged (see Figure 5a). This shift is influenced by the recovery rates: γ_{h_2}, which governs the transition from the quarantine compartment (Q_h) to the recovered compartment, and γ_{h_1}, which dictates recovery directly from the infected compartment to the recovered compartment. Since the recovery time is significantly longer in the quarantine compartment (Q_h), an increase in the number of individuals in Q_h leads to this observed shift.

When we simultaneously applied the three control parameters: v (vaccination), b (social distancing), and q (quarantine), we observed a significantly sharper reduction in the infected cases curve compared to when these controls were applied individually (see Figure 5b). The combined effect of these measures demonstrates the enhanced efficacy of a multi-faceted approach in the monkeypox outbreak mitigation. Specifically, when v and b are both greater

than 0.0025, and q exceeds 0.075, the number of infected cases is almost entirely eradicated. This finding underscores the importance of implementing these control measures together to achieve maximum suppression of disease transmission and highlights their combined impact on the control of monkeypox outbreaks.

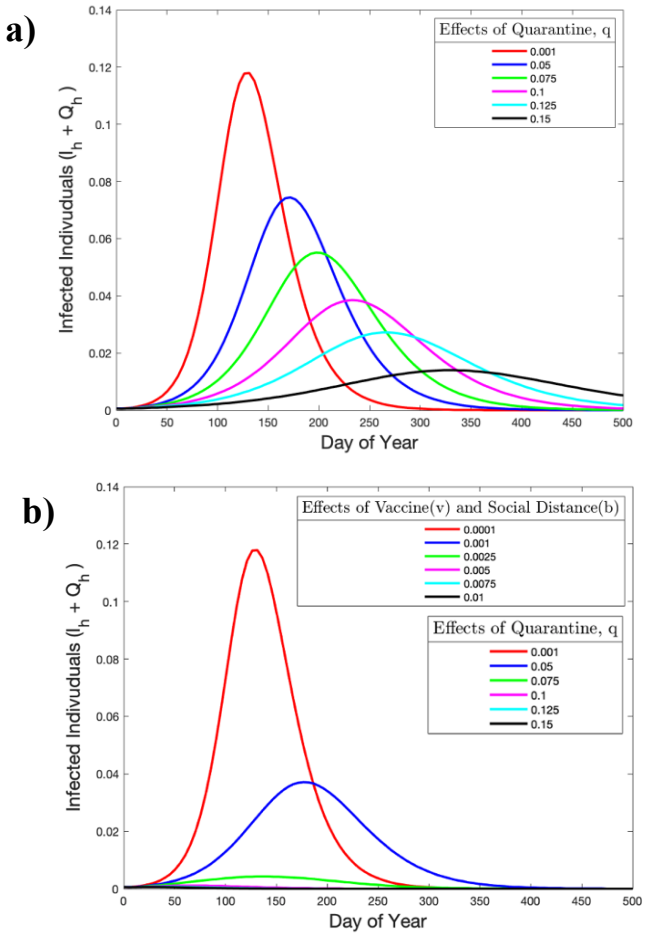

Figure 5. Plot a: the effect of quarantine on the infected cases. Plot b: the simultaneous combined effect of quarantine, vaccination and social distancing on the infected cases.

4 CONCLUSION AND SUGGESTIONS

In summary, our study provides a comprehensive analysis of the key parameters influencing the dynamics and control of the monkeypox outbreak, with a focus on stability analysis, sensitivity analysis, reproduction numbers, and the impact of control parameters. Stability analysis and Sensitivity analysis showed the importance of control parameters in the control of monkeypox outbreaks. Sensitivity analysis also revealed that parameters such as recovery rates and the incubation period play pivotal roles in shaping the outbreak trajectory. These findings highlight the importance of improving treatment quality and identifying infected

individuals quickly to mitigate disease spread effectively. Moreover, the significant role of human-to-human transmission (β_{hh}) compared to rodent-to-human transmission (β_{rh}) underscores the need for targeted interventions to disrupt transmission pathways most critical to the disease's basic reproduction number (R_0).

The investigation into the basic reproduction number further demonstrated that β_{hh} is nearly three times as influential as β_{rh} in determining R_0. This highlights the priority of focusing on human-to-human interactions when designing control strategies. Limiting direct transmission among individuals can have a far greater impact on reducing the overall spread than focusing on rodent-related transmission alone. Such insights are invaluable for allocating resources efficiently during an outbreak.

Finally, the analysis of control parameters v (vaccination), b (social distancing), and q (quarantine) emphasized their individual and combined effectiveness in reducing infected cases. While each parameter contributes meaningfully on its own, the simultaneous application of all three measures leads to a much sharper reduction in case numbers. Notably, when vaccination and social distancing parameters (v and b) exceed 0.0025, and the quarantine parameter (q) surpasses 0.075, the outbreak can be nearly eradicated. This demonstrates the power of a multifaceted approach, where integrating multiple control measures creates a synergistic effect, significantly enhancing outbreak mitigation.

In conclusion, our findings stress the necessity of a multifaced control strategy for the control of the monkeypox virus. By focusing on the most influential parameters and leveraging their combined effects, policymakers and health practitioners can design more effective interventions to manage and ultimately contain monkeypox disease outbreaks.

Conflict of Interest Statement

There is no conflict of interest between the authors.

Statement of Research and Publication Ethics

The study is complied with research and publication ethics.

Artificial Intelligence (AI) Contribution Statement

This manuscript was entirely written, analyzed, and prepared without the assistance of any artificial intelligence (AI) tools. All content, including text, data analysis, and figures, was solely generated by the author.

REFERENCES

[1] P. R. Reed et al., "Monkeypox virus transmission and pathogenesis," *Journal of Infectious Diseases*, 2004.

[2] Z. Jezek et al., "Human monkeypox," *American Journal of Tropical Medicine and Hygiene*, vol. 38, no. 2, pp. 3–13, 1988.

[3] S. S. Bhullar et al., "Emerging zoonotic viral diseases: Insights into monkeypox and its management," *Medical Research Reviews*, 2022.

[4] M. O. Sefiu, "Modeling the dynamics of rodent-human transmission of monkeypox using an SIQR-SEI framework," *Journal of Mathematical Epidemiology*, vol. 12, no. 3, pp. 256–271, 2024. *https://doi.org/10.38088/jise.1344860*

[5] P. Emeka, M. Ounorah, F. Eguda, and B. Babangida, "Mathematical model for monkeypox virus transmission dynamics," *Epidemiology*, vol. 8, no. 3, p. 1000348, 2018, doi: 10.4172/2161-1165.1000348.

[6] S. Somma, N. Akinwande, and U. Chado, "A mathematical model of monkeypox virus transmission dynamics," *Ife Journal of Science*, vol. 21, no. 1, pp. 195–204, 2019.

[7] Q. Huang, Y. Sun, M. Jia, M. Jiang, Y. Xu, L. Feng, and W. Yang, "An effectiveness study of vaccination and quarantine combination strategies for containing mpox transmission on simulated college campuses," *Infectious Disease Modelling*, vol. 9, no. 3, pp. 805–815, 2024, doi: 10.1016/j.idm.2024.04.004.

[8] M. S. Ullah and K. M. A. Kabir, "Behavioral game of quarantine during the monkeypox epidemic: Analysis of deterministic and fractional order approach," *Heliyon*, vol. 10, no. 5, p. e26998, 2024, doi: 10.1016/j.heliyon.2024.e26998.

[9] R. Alharbi, R. Jan, S. Alyobi, Y. Altayeb, and Z. Khan, "Mathematical modeling and stability analysis of the dynamics of monkeypox via fractional-calculus," *Fractals*, vol. 30, Art. no. 2240266, 2022, doi: 10.1142/S0218348X22402666.

[10] T. D. Frank, "Mathematical analysis of four SEIR-type models for monkeypox outbreaks: Human-animal interactions," *Mathematics*, vol. 12, no. 20, p. 3215, 2024, doi: 10.3390/math12203215.

[11] O. J. Peter, F. A. Oguntolu, M. M. Ojo, O. Abdulmumin, A. O. Oyeniyi, R. Jan, and I. Khan, "Fractional order mathematical model of monkeypox transmission dynamics," *Physica Scripta*, vol. 97, no. 8, p. 084005, 2022, doi: 10.1088/1402-4896/ac7ebc.

[12] O. I. Idisi, T. T. Yusuf, E. Adeniyi, A. A. Onifade, Y. T. Oyebo, A. T. Samuel, and L. A. Kareem, "A new compartmentalized epidemic model to analytically study the impact of awareness on the control and mitigation of the monkeypox disease," *Healthcare Analytics*, vol. 4, 2023, Art. no. 100267, doi: 10.1016/j.health.2023.100267.

[13] P. O. J. Peter, S. Kumar, N. Kumari, F. A. Oguntolu, K. Oshinubi, and R. Musa, "Transmission dynamics of Monkeypox virus: a mathematical modelling approach," *Model Earth Syst Environ*, vol. 8, pp. 3423–3434, 2022, doi: 10.1007/s40808-021-01313-2.

[14] R. Sah et al., "Monkeypox and its possible sexual transmission: Where are we now with its evidence?," *Pathogens*, vol. 11, no. 8, p. 924, 2022.

[15] P. van den Driessche and J. Watmough, "Reproduction numbers and sub-threshold endemic equilibria for compartmental models of disease transmission," *Mathematical Biosciences*, vol. 180, pp. 29–48, 2002, doi: 10.1016/S0025-5564(02)00108-6.

[16] O. Diekmann, J. A. P. Heesterbeek, and J. A. Metz, "On the definition and the computation of the basic reproduction ratio R_0 in models for infectious diseases in heterogeneous populations," *Journal of Mathematical Biology*, vol. 28, no. 4, pp. 365–382, 1990.

[17] O. I. Idisi and T. T. Yusuf, "A mathematical model for Lassa fever transmission dynamics with impacts of control measures: Analysis and simulation," *European Journal of Mathematics and Statistics*, vol. 2, no. 2, pp. 19–28, 2021, doi: 10.24018/ejmath.2021.2.2.17.

[18] E. J. Routh, *A Treatise on the Stability of a Given State of Motion, Particularly Steady Motion*. Cambridge, UK: Cambridge University Press, 1877.

[19] A. Hurwitz, "Ueber die Bedingungen, unter welchen eine Gleichung nur Wurzeln mit negativen reellen Theilen besitzt," *Mathematische Annalen*, vol. 46, no. 2, pp. 273–284, 1895, doi: 10.1007/BF01446812.

[20] G. Chowell, H. Nishiura, and L. M. A. Bettencourt, "Comparative estimation of the reproduction number for pandemic influenza from daily case notification data," *Journal of Theoretical Biology*, vol. 364, pp. 149–159, 2014, doi: 10.1016/j.jtbi.2014.08.004.

[21] I. H. Aslan, M. Demir, M. M. Wise, and S. Lenhart, "Modeling COVID-19: Forecasting and analyzing the dynamics of the outbreak in Hubei and Turkey," *Mathematical Methods in the Applied Sciences*, vol. 45, no. 10, pp. 6481–6494, 2022, doi: 10.1002/mma.8181.

[22] M. Demir, I. H. Aslan, and S. Lenhart, "Analyzing the effect of restrictions on the COVID-19 outbreak for some US states," *Theoretical Ecology*, vol. 16, pp. 117–129, 2023, doi: 10.1007/s12080-023-00557-1.

[23] S. Marino, I. B. Hogue, C. J. Ray, and D. E. Kirschner, "A methodology for performing global uncertainty and sensitivity analysis in systems biology," *Journal of Theoretical Biology*, vol. 254, no. 1, pp. 178–196, 2008.

[24] H. Joshi, M. Yavuz, S. Townley, and B. K. Jha. "Stability analysis of a non-singular fractional-order covid-19 model with nonlinear incidence and treatment rate". *Physica Scripta* 98.4 (2023): 045216.

[25] H. Joshi. "Mechanistic insights of COVID-19 dynamics by considering the influence of neurodegeneration and memory trace", *Physica Scripta* 99.3 (2024): 035254

[26] H. Joshi, and M. Yavuz. "Transition dynamics between a novel coinfection model of fractional-order for COVID-19 and tuberculosis via a treatment mechanism". *The European Physical Journal Plus* 138.5 (2023): 468.

[27] H. Joshi, and B. K. Jha. Fractional reaction diffusion model for parkinson's disease, Proceedings of the International Conference on ISMAC in Computational Vision and Bio-Engineering 2018 (ISMAC-CVB). Springer International Publishing, 2019.